

Dielectric and impedance spectroscopy investigations on highly structured corrosion protection coatings on mild steel

S. Schmitz-Stoewe, M. Jochum, S. Albayrak, E. Perre, M. Wild, C. Becker-Willinger, INM – Leibniz Institute for New Materials, Saarbruecken/Germany

Summary

Highly structured composite coatings derived from epoxy phenolic resin matrix with dispersed platelet shaped SiO₂ type fillers with high aspect ratio have shown interesting dielectric behavior at low filler concentration up to 10 wt.-% already in the past. The observations made so far indicated that dispersion of the platelets with aspect ratio of about 30 and the use of special orientation additive increased the cross-linking density of the matrix as well as of the resulting composite coatings. In the present investigation the filler content of the composites was increased in a stepwise manner up to 40 wt.-% of platelet particles in order to elucidate the limiting degree of filling. The morphological analysis by means of metallographically prepared cross-sections of coatings on steel in combination with scanning electron microscopy (SEM) revealed that the orientation and the alignment of the platelets seemed to be mainly determined by the filler concentration in combination with orientation additive. The morphological findings directly correlated with the barrier properties detected in the electrochemical impedance spectroscopy (EIS) analysis. Dielectric (DE) spectroscopy measurements in dependence on the temperature showed that extreme degrees of filling with platelets might have an influence on the curing behavior of the matrix. The localized corrosion processes in these highly filled composite coatings were analyzed using scanning vibration electrode technique (SVET). The maximum degree of filling of 40 wt.-% enabled to extend the stability of the coatings when applied on mild steel up to 1000 h in the neutral salt spray test.

1 Introduction

Corrosion protection on mild steel is realized by many different approaches such as zinc containing coating layers [1, 2], organic coating layers containing corrosion inhibitors [3, 4] as well as by efficient barrier coatings [5]. The focus of our own investigations laid on the morphology of highly structured corrosion protection coatings on mild steel composed of an epoxy-phenolic resin matrix in combination with anisotropic platelets and orienting additive [6]. As a basis of the actual work it was already reported about compositions containing low platelet amounts of 0, 2, 5 or 10 wt.-% and 0, 1 or 2 wt.-% of orienting additive [7]. It could be shown that besides the alignment of platelets which leads to a higher physical barrier according to the Nielson theory [8], the orienting additive is also responsible for an increased cross-linking of the matrix which results in a higher corrosion protection effect. In order to clearly distinguish between the two structural conditions it would be important to identify the key properties of the used platelets regarding their surface chemistry, their morphological arrangement over the polymer matrix including their influence on the resulting cross-linking density of the matrix. The present paper tries to correlate the specific microstructural factors in composite coatings with their corrosion protection ability and barrier function by forcing the alignment of platelet type particles by increasing the amount to maximum extent possible that still allows quite simple application as well as by further addition of orienting additive.

2 Experimental

2.1 Materials

Mild steel substrates (ST1203, 10 x 10 x 0.1 cm) were cleaned by degreasing in acetone, followed by 15 min at 70 °C ultrasonic treatment with alkaline Surtec-cleaners 138 (5 %) and 089 (0.5 %), rinsing with deionized water and finally drying at a high pressure airstream. To minimize intermediate corrosion the samples were cleaned immediately before coating. All chemicals used were of analytical grade and used without further purification. Epoxy resin BECKOPOX[®]EP307 [= EP307] and phenolic resin PHENODUR[®]PR722/53BG/B [= PR722] were both from Cytec Surface Specialties Germany GmbH & Co KG; solvent n-Butyl acetate [= BA] from Sigma Aldrich, orienting additive Ceratix 8461 [= CT] from BYK-Chemie GmbH, platelets Colorstream[®] T20-04 WNT Lapis Sunlight [= LS] from MERCK KGaA PLS/Pigments.

2.2 Synthesis procedure of coating lacquer material

All coating materials were composed on base of an epoxy-phenolic resin matrix (EP307 + PR722) in combination with different amounts of platelets (LS) and orienting additive (CT). The matrix forming components were mixed by using a Dispermat[®] with dispersion impeller and Silibeads. First EP307 was dissolved in BA to obtain a processable solution having 33 wt.-% solid content. Then PR722 was added resulting in a wt.-% ratio of 80:20 EP307:PR722. The orienting additive CT has been added in an amounts of 2 wt.-%. After the Silibeads have been removed platelets LS were added in concentrations of 10, 20, 30 and 40 wt.-% and a homogeneous dispersion was formed using a dissolver disc.

2.3 Preparation of coating layers

The coating layers were prepared on 10 cm x 10 cm mild steel substrates (ST1203) by coating with a Quadruple Film Applicator (film width 90 mm), Model 360 from Erichsen GmbH & Co.KG with a gap clearance of 150 µm in combination with a ZAA 2300 Automatic Film Applicator Coater from Zehntner GmbH Testing Instruments using a drawing speed of 9 mm/s. For curing a circulating air drying cabinet from HERAEUS Instruments / Thermo Scientific type WU 6100 was used. The coated substrates were cured in laying position in a temperature program up to 200 °C.

2.4 Testing Methods

All measurements were performed on cured coating materials. The average roughness Ra of the coated surfaces was investigated by a Perthometer M1 from Mahr GmbH. For determination of the coating thickness a Fischerscope MMS Permascope[®] and for examination of micro-hardness according to DIN EN ISO 14577 a Fischerscope Hm2000 were used. The coating morphology was determined by Scanning Electron Microscopy (SEM), using a Quanta 400 F (FEI-Company) in the low vacuum modus (100 Pa) at 20.0 kV on polished in epoxy resin embedded cross-section samples. Broadband dielectric spectroscopy (DE) was performed using an Alpha-A high performance frequency analyzer with active sample cell, version V4.1ANB from Novocontrol Technologies GmbH in two parallel electrode configuration. The DE spectra were recorded in the frequency range from 0.1 Hz to 1 MHz at temperatures from 0 °C to 80 °C in 10 °C steps under an AC field of 1 V. Electrochemical impedance spectroscopy (EIS) measurements were carried out using a SP240 Potentiostat / Galvanostat / FRA from BioLogic in a three-electrode arrangement cell containing deionized water with 3.5 wt.-% NaCl as electrolyte. The working electrode was the sample (exposed area 7.068 cm²), the counter electrode was a Pt coil and the reference electrode was Ag/AgCl in 3.0 M NaCl (0.209 V vs.

NHE). Impedance spectra were investigated from 1 MHz to 10 mHz with a 10 mV sine wave voltage amplitude. Neutral salt spray corrosion test (NSS) was performed according to DIN EN ISO 9227 in a corrosion testing apparatus, model 606/400 I provided by Erichsen GmbH & Co KG. The salt spray solution was a (50 ± 5) g/l NaCl in water with a pH of 6.5 to 7.2 at (25 ± 2) °C, which was sprayed into the test chamber at (35 ± 2) °C. The samples were investigated up to 1008 h and controlled in intermediate steps. SVET-measurements were performed with a SVP 100 KV system from Princeton Applied Research. On the samples an artificial scratch of 4 mm down to the bare steel was applied with a scalpel. The scratched sample was mounted in a non-earthed configuration and used as working electrode (WE). Pt/Ir-alloy was used as testing probe, fixed at a small fixed distance to this sample. In this non-earthed sample configuration glassy carbon was used as earthed counter electrode (CE). Electrolyte was 0.01 wt.-% NaCl-solution ($\sim 330 \mu\text{S}/\text{cm}$; ~ 25 °C). The measurement was performed with open circuit potential over a time period of 24 h in sweep mode and peak-to-peak amplitude of $30 \mu\text{m}$ at a frequency of 81 Hz.

3 Results and discussion

In order to build the composites for protective coatings an epoxy phenolic resin copolymer having a weight ratio 80:20 was used as matrix system. Platelets were added in concentrations of 10, 20, 30 and 40 wt.-% to investigate the effect of barrier functionality in comparison to the unfilled matrix. In order to elucidate the effect of degree of alignment of the platelets on the barrier and corrosion protection properties, all the coatings from above containing platelets were prepared using an orienting additive in concentrations of 0 and 2 wt.-%. As a further reference system the pure matrix has with 2 wt.-% orienting additive as well. All compositions prepared are listed in Table 1.

Table 1: Investigated compositions of composite coatings having matrix EP307:PR722 80:20 containing different amount of platelets (LS) and orienting additive (CT).

sample	LS [wt.-%]	CT [wt.-%]	sample	LS [wt.-%]	CT [wt.-%]
PS-00-0	0	0	PS-00-2	0	2
PS-10-0	10	0	PS-10-2	10	2
PS-20-0	20	0	PS-20-2	20	2
PS-30-0	30	0	PS-30-2	30	2
PS-40-0	40	0	PS-40-2	40	2

The resulting liquid reaction mixtures were applied on mild steel plates using raking technique and were cured in a temperature program up to 200 °C. All liquid coating materials were applied with a film coater having a gap clearance of $150 \mu\text{m}$. The same wet coating thickness led to slightly differing values of the dry coating thickness in the average range of $36.4 \mu\text{m} \pm 5.9 \mu\text{m}$ for all compositions.

3.2 Morphology

The composites were designed to be prepared up to high loading levels of platelets in order to study the dependence of platelet alignment ability under confined space conditions at least for the highest concentrations achievable. As the role of orienting additive should be dependent on the geometric, electronic and supramolecular conditions and cannot be predicted for new compositions, its concentration influence was investigated as well. The resulting morphology and platelet distribution over the

matrix was examined using SEM on polished cross-sections. Figure 1 shows the resulting micrographs for the coating systems PS 10-x and PS 40-x with x =0 and x = 2, respectively.

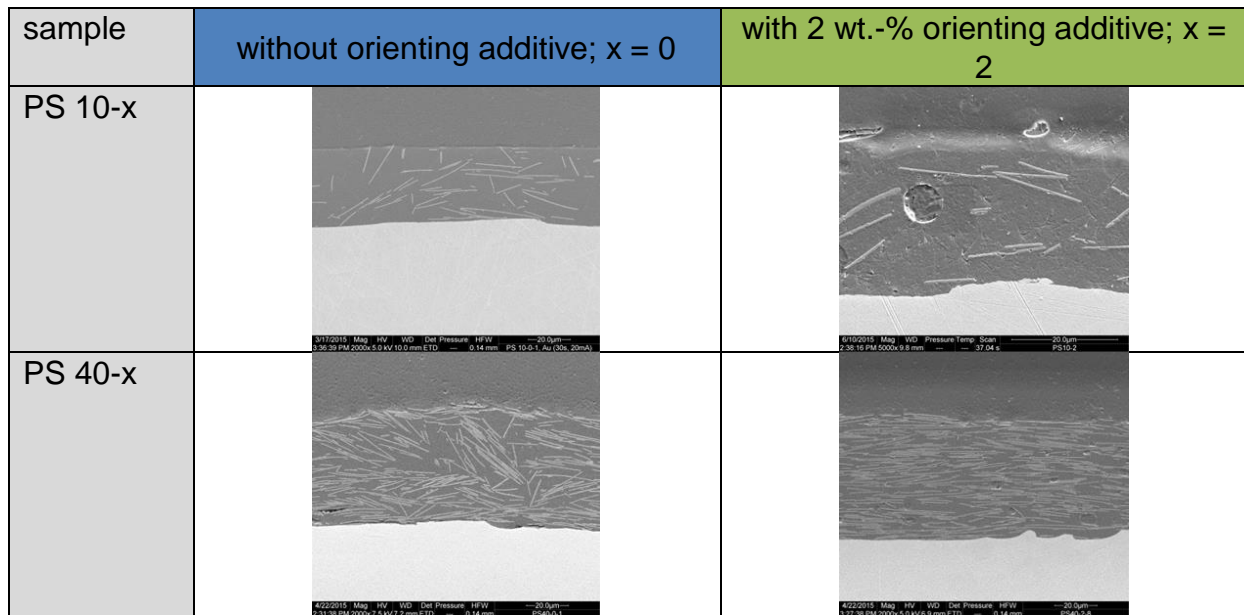


Figure 1: SEM micrographs of coatings with different amount of platelets and orienting additive

At low platelet content with or without orienting additive (PS 10-2 and PS 10-0) no orienting effect can be detected. But it is obvious that when the platelet amount is too low compared to the used amount of CT, the additive can separate in form of droplets from the matrix material and by this way will not significantly influence the platelet orientation. In SEM images of coatings with high amounts of platelets (40 wt.-%) the influence of orienting additive for the composite is visible. With orienting additive (PS 40-2) the platelets are highly oriented parallel to the substrate, whereas without additive, a more randomly oriented distribution is achieved.

3.3 Surface Roughness

As the incorporated platelets have anisotropic shape, it was supposed that the average coating roughness could depend on their amount and orientation in the coating.

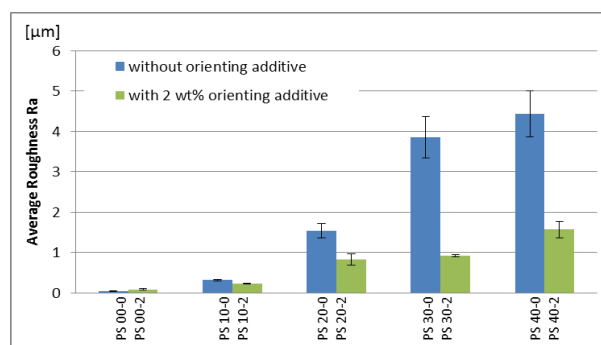


Figure 2: Average coating roughness R_a of cured composite coating materials

As can be derived from figure 2 using no orienting additive led to a strong increase in average roughness R_a with increasing amount of platelets. However using 2 wt.-% of orienting additive leads to much smoother surfaces and less pronounced increase in surface roughness with increasing platelet concentration. An explanation for this can

be given by the morphology investigations (figure 1) of the platelet orientation in the matrix material. The platelet orientation in compositions with 2 wt.-% additive is highly aligned and shows a roof tile arrangement. Especially in compositions with high amount of platelets this effect is demonstrative and leads to a smooth surface where no platelets poke out of the coating surface or form disordered agglomerates.

3.4 Micro-hardness

Coating materials without orienting additive were composed from relatively soft polymer matrix and rigid particles platelets both having different elastic modulus and hardness. For this reason it was of interest to follow the increase of hardness of the coating surface in dependence on the platelet filler content.

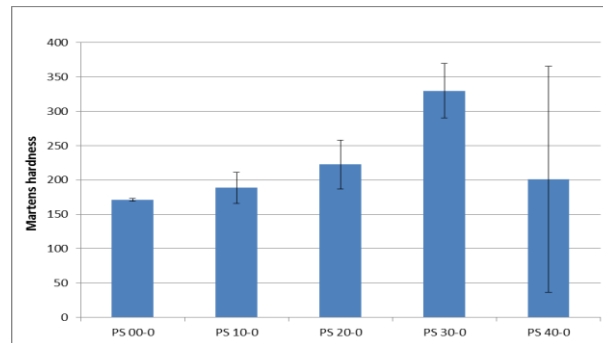


Figure 3: Martens hardness of composite coatings on steel.

When looking at the average values of Martens hardness an increase can be detected with increasing amount of platelets. This would also be expected from a simple rule of mixture behavior. For the coating system containing 40 wt.-% platelets the Martens hardness decreased again. This behavior might be a hint that the coating material gets brittle when using a very high amount of platelets. One reason for this could be that the remaining matrix ligaments may become too thin in order to exhibit sufficient load bearing capacity by losing the ability of controlled crack propagation. This observation is in accordance with the findings in the morphological analysis, which shows the occurrence of matrix ligaments with only several hundreds of nanometers in thickness.

3.5 Neutral Salt Spray Test (NSS)

NSS test was used to obtain information about corrosion protection in dependence on the coating composition. After applying an artificial notch of 0.5 mm width through the coating up to the steel surface the NSS-test has been done for 1000 h. Results of the corrosion tests are shown in figure 4 for coating systems containing 0; 10 and 40 wt.-% platelets and 0 as well as 2 wt.-% orienting additive, respectively.



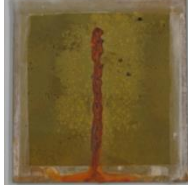









PS 00-0		PS 00-2	
			
view on coating: blistering and pitting corrosion	subsurface migration: complete delamination and formation of corro- sion products	view on coating: blistering and pitting corrosion	subsurface migration: complete delamination and formation of corro- sion products
PS 10-0		PS 10-2	
			
view on coating: no change in surface; start blister formation on notch	subsurface migration: almost complete de- lamination	view on coating: no change on surface; stronger blistering at notch	subsurface migration: complete delamination
PS 40-0		PS 40-2 after	
			
view on coating: no corrosion over sur- face detectable	subsurface migration: Subsurface Migration $W_b^{(*)} = 9$ mm; remain- ing coating still intact	view on coating: no corrosion over sur- face detectable	subsurface migration: Subsurface Migration $W_b^{(*)} = 8$ mm; remain- ing coating intact

Figure 4: View on coatings and subsurface migration after 1008 h NSS on mild steel ST 1203.

(*) Calculation of subsurface migration $\frac{(\text{average value of delamination width} - \text{notch width})}{2}$

After 1008 h of NSS testing it can be observed that for all the unfilled matrices and the composites with low amount of platelets (10 wt.-%) formation of blisters and pitting corrosion occurred at the artificial notch and also on the plane area, indicating that the materials are saturated with sodium chloride solution leading to a partial delamination all over the surface. A total subsurface migration including complete delamination of coating material has taken place. Mechanical removal of the coating with a plastic spatula revealed for PS 10-x in contrast to PS 00-x that there is no corrosion occurring at the steel surface beneath the notch. An amount of 40 wt.-% of platelets in the coatings led to avoidance of blister formation on the plane area. Red rust is obviously formed in the artificial scribe but not on other areas of the coated plates. Subsurface migration can be determined after removing the delaminated areas and calculated according to the equation (*) given above.

In this macroscopic testing there is no great difference observable with respect to subsurface migration neither with orienting additive nor without. The corrosion protection effect is strongly depending of the amount of platelets used in the coating material.

3.5 Electrochemical Impedance Spectroscopy (EIS)

In experimental arrangements for EIS measurements the complex impedance $Z(j\omega) = Z' + jZ''$ can be presented as complex plane plots of real part Z' versus imaginary part Z'' (Nyquist plot). The capacitance and resistance of a system can be determined by fitting the Nyquist plot with components of an electric circuit. The capacitance of the coating can be directly linked to its permeability. An increase of capacitance can be associated to an increased permeability of the coating. Figure 5 shows the fitted capacitance of coatings with and without orienting additive.

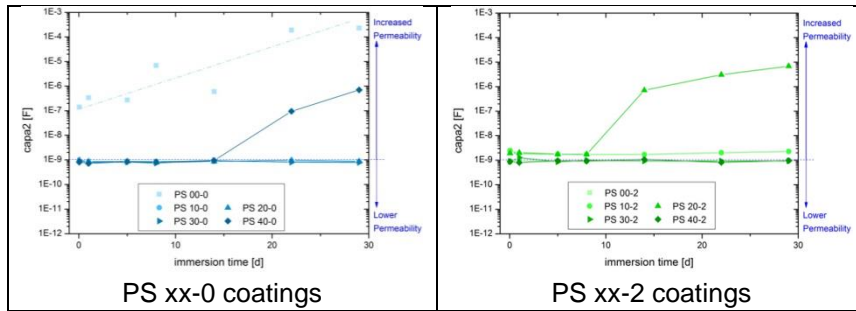


Figure 5: Capacitance in dependence of immersion time showing permeation effects through the coating material

Coating materials containing platelets without orienting additive show low permeability. At 40 wt.-% platelet concentration the material is getting permeable after 14 days, which can be detected by an increase in the capacitance part. The coating material without platelets and without orienting additive (PS 00-0) shows a higher capacitance value right from the start of the measurement. This might be due to the fact, that this coating material has pores or that the corroding medium is diffusing very easily through the coating. With 2 wt.-% of orienting additive all coating materials show low permeability. This might be due to the observed levelling effect, produced by the additive. PS 20-2 shows an increase in permeability after 8 days which may be caused by insufficient distribution of orienting additive in the coating layer.

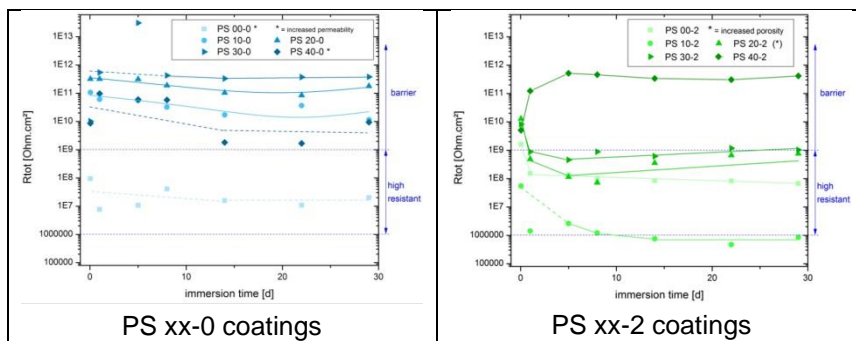


Figure 6: Total resistance in dependence of immersion time showing resistance effects in the coating material.

The increased porosity of coating material without platelets and no orienting additive (PS 00-0) is reflected by the total resistance of the material in figure 6. It only shows high resistance (range between $10^6 \Omega \cdot \text{cm}^2$ - $10^9 \Omega \cdot \text{cm}^2$), whereas all other coatings with platelets and no orienting additive are real barrier materials (total resistance $> 10^9 \Omega \cdot \text{cm}^2$) [9]. The hints given by micro-hardness and the determination of porosity that the coating with the highest platelet amount PS 40-0 may have intrinsic defects

can also be found in the diagram. Whereas the barrier properties continuously increase with increasing platelet amount, that coating PS 40-0 has less barrier properties. With 2 wt.-% of orienting additive the total resistance of all coating materials except of PS 40-2 lays in the range of high resistance materials ($10^6 \Omega\cdot\text{cm}^2 - 10^9 \Omega\cdot\text{cm}^2$). The only coating material with barrier properties ($> 10^9 \Omega\cdot\text{cm}^2$) is here the coating PS 40-2. From EIS measurements it can be concluded that coatings without orienting additive show better corrosion resistance properties than coatings with orienting additive. These EIS results are not reflecting the NSS results, because in EIS all samples with 10 to 40 wt.-% of platelets and 0 wt.-% of orienting additive show real barrier properties with total resistances greater than $10^9 \Omega\cdot\text{cm}^2$, but in the NSS test the compositions with low amount of platelets failed. A possible explanation may be that in contrary to NSS test the samples for EIS were not artificially scratched and the test is less aggressive. So this allows the assumption that in NSS test besides the corrosion processes also delamination processes along the notch play an important role in the corrosion protection behavior. In this direction further investigations have to be performed.

3.6 Scanning Vibration Electrode Technique (SVET)

Furthermore it was of interest to obtain information on the local corrosion propagation behavior at an artificial damage that has been applied on the coating. This investigation was performed using SVET (see figure 7).

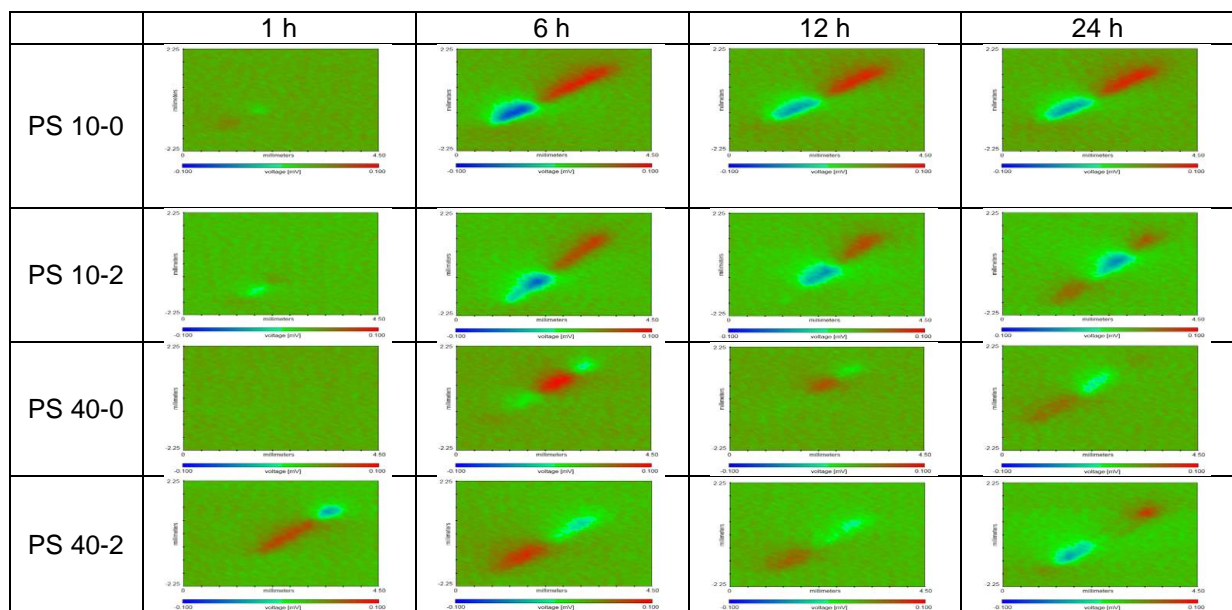


Figure 7: SVET measurements for selected composite coatings (anodic areas: blue; cathode areas: red)

From the SVET diagrams the maximum anodic corrosion potential was determined and its change over time was plotted in order to get information about the corrosion process of the point where the corrosion process started and the strongest corrosion process is located.

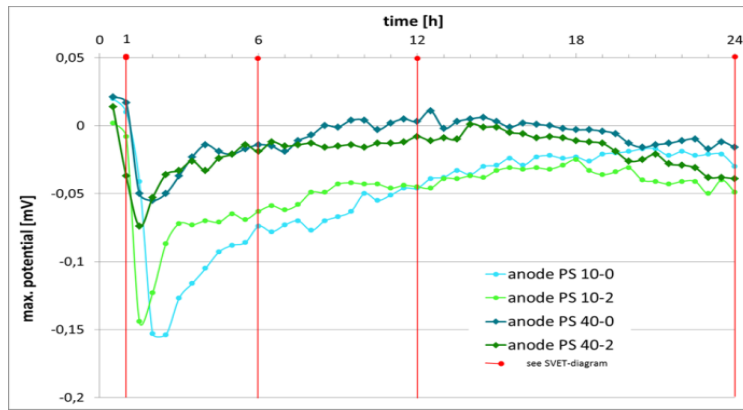


Figure 8: Maximum anodic potential derived from SVET measurements for selected composite coatings

The measured maximum anodic potential values, which are indicating the proceeding of the corrosion process, are reached at different times depending on the amount of orienting additive. With orienting additive (PS 10-2 and PS 40-2) the most negative value of the curves is reached earlier than without orienting additive (PS 10-0 and PS 40-0). The amount of platelets has an influence on the extent of the measured anodic potential. For coatings with 40 wt.-% of platelets the value is not as negative as for 10 wt.-% of platelets. This may be a hint to the fact that the corrosion process is not so strong for composite coatings containing 40 wt.-% of platelets.

3.7 Dielectric behavior

In order to detect phase transitions like glass transitions as well as the general behavior over a broader frequency range the dielectric behavior of fully cured composite coatings was investigated using DE spectroscopy. Figure 9 shows the real part ϵ' of the complex dielectric permittivity and the dielectric loss factor $\tan \delta$ for the unfilled matrix and the composite material containing 40 wt.-% platelets both with 2 wt.-% orienting additive in dependence on frequency and temperature.

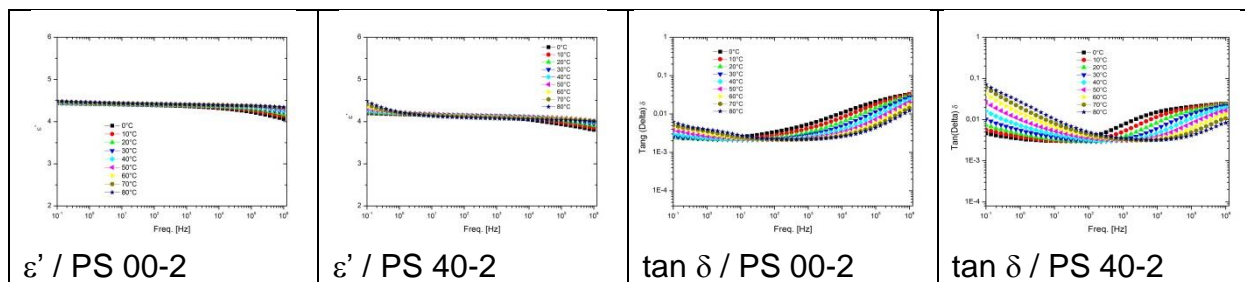


Figure 9: real part ϵ' of the complex dielectric permittivity and the damping behavior $\tan \delta$ in dependence on the frequency and temperature.

As can be derived from figure 9 the real part ϵ' of the complex dielectric permittivity for both systems is almost unaffected by the change in frequency and temperature indicating that the polarization is kept. On the other hand the dielectric loss factor $\tan \delta$ shows significant temperature dependence in the investigated frequency range. The relaxation polarization frequency (= cross-over point between the different isotherms) is shifting towards higher frequency when 40 wt.-% of platelets are added. At the same time the relaxation extent at 10^{-1} Hz increases from about 0.002 to only 0.007 for PS 00-2 and from about 0.004 to almost 0.08 for PS 40-2 indicating

interaction between platelet surface and polymer matrix. On the other hand the temperature dependence and absolute value of $\tan \delta$ above 10^3 Hz are almost similar for both systems. Below 10^3 Hz PS 40-2 shows a stronger broadening in relaxation signals in dependence on temperature compared to PS 00-2. The observations could indicate that the matrix in system PS 40-2 is less cross-linked in extent compared to PS 00-2 due to confined space conditions (see figure 1). This reduced extent of matrix curing would also explain the behavior observed for PS 40-x in the Martens hardness, which deviated from the simple rule of mixture that is suggested in figure 3 and showed an unexpected decrease when going from 30 wt.-% to 40 wt.-% platelets.

4 Summary and conclusion

Composite coatings based epoxy-phenolic matrix with amounts of SiO₂ platelets up to 40 wt.-% and average dry film coating thickness $36 \pm 6 \mu\text{m}$ were applied on mild steel (ST 1203). Addition of orienting additive especially for compositions with 40 wt.-% platelet content led to a roof tile arrangement for platelets with matrix ligaments having low thickness (confined space conditions). Neutral salt spray test revealed improved corrosion resistance with increasing platelet content whereas the concentration of the orienting additive had almost no influence. A similar tendency could also be found in the SVET measurements. EIS on the other hand revealed barrier functionality for high platelet content in presence of orienting additive. DE spectroscopy indicated incomplete matrix curing under confined space conditions when analyzed on the low frequency end which seems to be in accordance with the observed behavior of the Martens hardness for extreme platelet contents. A more detailed analysis of these observations will be part of future investigations.

5 Acknowledgments

The authors wish to thank Ms. B. Heiland for the very skilled preparation of the polished cross-sections and the SEM analysis.

6 References

- [1] Shreepathi, S., Bajajaj, P., Mallik, B.P.; *Electrochimica Acta* **55**; 5129-5134 (2010)
- [2] Barcelò, G., Sarret, M., Müller, C., Pregonas, J.; *Electrochimica Acta* **43**; 13-20 (1998)
- [3] Hackerman, N.; *Materials Performance* **29**; 44-47 (1990)
- [4] Chang, C.M., Yeh, J.M.; *Advanced Materials Research* **747**; 35-38 (2013)
- [5] Dong, Y., Ma, L., Zhou, Q.; *J. of Coatings Technol. Research* **10**; 909-921 (2013)
- [6] Schmitz-Stöwe, S., Opsölder, M., Jochum, M., Aslan, M., Becker-Willinger, C., EURO-CORR 2012, September 09-13, 2012, Istanbul , (2012)
- [7] Becker-Willinger, C., Schmitz-Stoewe, S., Opsoelder, M., Jochum, M., Albayrak, S., Perre, E., EUROCORR 2014, September 08-12, 2014, Pisa , (2014)
- [8] Nielsen, L. E.; *J. of Macromolecular Science A* **1**; 929-942 (1967)
- [9] Amirudin, A.; Thierry, D.; *Progress in organic coatings* **26** 1-28 (1995).